Presented at the Intl. KEK Workshop on Kaon, Muon, Neutrino Physics and Future, October 31 - November 1, 1997, Tsukuba, Japan

BNL-65258

CONF-9710190--

Evidence of $K^+ \to \pi^+ \nu\bar{\nu}$: The BNL E787 1995 result (How did we get here) *

I-Hung Chiang
Brookhaven National Laboratory, upton, NY 11973, USA
for the BNL E787 collaboration *

1 Introduction

The kaon was studied very thoroughly since its discovery some 50 years ago. In the study of charged kaon branching ratios, it was noticed that $K^+ \to \pi^0 e^+ \nu_e$ is allowed while $K^+ \to \pi^+ \nu\bar{\nu}$ is not. The latter was then empirically classified as a forbidden decay, leading to the so-called 'strangeness-changing current' rule. The decay $K^+ \to \pi^0 e^+ \nu_e$ is mediated by the 'strangeness-changing charged current' and its branching ratio is 4.8 %. By contrast $K^+ \to \pi^+ \nu\bar{\nu}$ is a 'strangeness-changing neutral current', which is 'forbidden'. In 1970, the GIM model [1] was introduced to explain this effect and in 1974, Gaillard and Lee [2] calculated the $K^+ \to \pi^+ \nu\bar{\nu}$ branching ratio to be on the order of 10^{-10}. In the current theory, the $K^+ \to \pi^+ \nu\bar{\nu}$ is mediated by a Flavor Changing Neutral Current (FCNC) in which the cancellation of the three quark generations should be complete down to second order except for the difference in the quark masses. The top quark is much heavier than the charm and up quarks, so that the cancellation is not complete. In other words, this decay is more dependent on the top sector. The measurement of $K^+ \to \pi^+ \nu\bar{\nu}$ branching ratio measures the modulus of the V_{td} element of the CKM Matrix. The 1995 results of E787 were published in 1997 [3]. This report is focused on how we achieve the goal of detecting events with such as small branching ratio.

2 Experimental Method

E787 was proposed in 1983. We decided to take advantage of the properties of decay at rest. Fig 1 shows the branching ratios and charged daughter momentum distributions of the 7 major decay modes of K^+. Also included are the expected branching ratio and momentum distribution of $K^+ \to \pi^+ \nu\bar{\nu}$. These major modes have to be eliminated down to a branching ratio level of 10^{-11}, *i.e.* 10 times below the signal level. We decided to confine our search to the momentum region between $K^+ \to \pi^+ \pi^0$ and $K^+ \to \mu^+ \nu_\mu$ (205 Mev/c < P < 235 Mev/c). There is no

*Worked performed under the auspices of the U.S. Dept. of Energy.

π^+ from the major modes in this region. The measurement of the charged track momentum provides a large rejection against those modes with π^+. In addition, there is almost always a π^0 accompanying the π^+. Thus the photon veto provides additional rejection. The modes with leptons are suppressed by the pion particle ID from the $\pi \to \mu \to e$ life cycle. The photon veto and kinematics provided additional suppression against the leptonic modes. Two previous experiments [4], [5] used a similar strategy but ours is more ambitious, aimed to reject background down to 10^{-11}. The E787 detector is shown in Fig. 2 [6]. It was designed to achieve the following goals.

- Measure all properties of the charged particle.

  1. Use a separated beam to enhance the purity of the kaon beam and use a Čerenkov counter to further identify the incident particles.
  2. Beam chambers measured the incident direction.
  3. Enclose the decay region with a 1 Tesla field and surround the 'target' with a cylindrical drift chamber so the momentum and the direction of the charged particle can be measured.
  4. Energy and range were measured by the active scintillating range stack (RS) and the scintillating fiber target.
  5. The two range stack chambers measured the charge particle direction inside the Range Stack.

- Fully active photon veto.

  1. Lead scintillator barrel veto. Detects γ's in directions transverse to the incident beam.
  2. Lead scintillating end cap. Detect γ's in the forward and backward direction of the incident beam.
  3. The active fiber target and range stack also detect γ's.

- Active scintillation fiber target.

  We used the active fiber target as a "target" to stop the kaon. This enabled us to study the decay topology. Each fiber was equipped with TDCs and ADCs. The timing of each fiber allowed us to identify source of the signal. The energy loss of the pion in the stopping target was properly accounted for in calculating its initial momentum.

- Particle ID.

  The stopping layers of the range stack were instrumented with 500 MHz Transient Digitizer to digitize the $\pi \to \mu \to e$ decay sequence. Fig 3 shows the time history of both the upstream and downstream views of layer 11 to 14. Layer

12 is the stopping layer which shows the $\pi \rightarrow \mu \rightarrow e$ time sequence. Layer 11 shows only the pion and Layers 13 and 14 show only the decay electron.

3 Pre-1995 data taking

The first data run was done with partially instrumented detector in 1988. The run yielded a single event sensitivity of 1.4×10^{-8}. The subsequent runs, 1989 - 1991, were taken with the full detector, using the LESBI (Low Energy Separated Beam I) and yielded a single event sensitivity of $\sim 1.0 \times 10^{-9}$, We learned from the data that that we had to upgrade our detector/beam system. The goal was a ten-fold improvement in our sensitivity/year. The limiting factors were:

- Kaon Beam intensity and purity
    1. LESBI Beam Acceptance: Acceptance of the LESBI is 12.1 msr-% with $10.5^{o} \pm 1.65^{o}$ production angle. By increasing the solid angle and reducing the production angle should substantially increase the K^{+} flux in the beam line.
    2. Separator: LESBI is a Single stage separated beam. The beam purity is $\pi^{+} : K^{+} = 3 : 1$. A two stage separated beam, like the BNL 2-Gev beam, will improve the beam purity.
    3. Production Target: The primary beam intensity limit on the C target is 10 TP. The limit is due to insufficient cooling of the Platinum target.
    4. Primary Beam: AGS total beam intensity was less than 20 TP (TP=10^{12} protons).
- Data Acquisition: The system bandwidth was reaching its maximum, with VAX, 9-track magnetic tape etc. We needed to modernized the system to accommodate the order of magnitude increase in data rate.
- Detector: The following detector upgrades were deemed desirable/reasonable.
    1. Drift Chamber: Improve the drift chamber will reduce the error of the momentum measurement.
    2. Range Stack: Demultiplex the inner layers of the RS counters will increase the light collection and improve the energy resolution of the Range Stack.
    3. Range Chamber: Replacing the chamber by straw tube chamber will reduce the dead material in the range stack and improve the energy resolution.
    4. Photon veto: Better detector in the End Caps will reduce the dead time due to accidental veto. Effective denser material will reduce photon leakage in the overlap region, between Barrel veto and end cap.

5. Target Fibers: Improve the light output of the fibers will improve the timing, energy resolution and the pattern recognition in the stopping target region.

6. DAQ: Improve the rate capability of the system, both in DAQ and signal processing will reduce system dead time and improve data taking efficiency,

4 Upgrades

The planned Booster construction was finished by the end of 1992. The intensity of AGS was quadrupled. Fig. 4 shows the time line of the proton intensity with various AGS upgrades. On the other hand, it was still short of the factor of 10 increase we needed. In addition, it is not desirable to increase the rate in the detector by factor of 10. It was decided that a new separated beam should be built. The new beam is a two stage separated beam with a factor 4 increase in acceptance and much greater purity, $K^+ : \pi^+ \approx 3 : 1$ (LESBI I $K^+ : \pi^+ = 1 : 3$). With more beam on target and the better K/pi ratio, the detector could be run with 10 times more K^+ incident without substantially increasing the rate in various subsystems. Fig. 5 shows the layout of the new beam. Table I shows comparison of the old beam (LESBI) and the new beam (LESBIII).

Table I Comparison of old and new beam

Item	LESBI (old)	LESBIII (new)
Maximum Momentum	800 Mev/C	830 Mev/C
Production Angle	10.5^o	0^o
Solid Angle	2.6 msr	12 msr
$\Delta P/P$	4 %	4 %
Beam Line Length	15 meter	19.6 meters
Separator	Single stage	Two stages
	10.2 cm gap 575 KV, 2 meters	10.2 cm gap 560 KV, 2 meters
		12.7 cm gap 625 KV, 2 meters
Production Target (Platinum)	8.9 cm air cooled	6 cm water-cooled
Maximum Proton Beam On Target	10 TP	> 30TP
Vertical Mass Slit	1	2
Momentum Jaw	1	1
4 Jaw Θ-Φ Collimator	0	1
Horizontal Collimator at Achromatic Focus	0	1
Beam Purity π/K	3/1	1/3

The intensity limit of the original production target was due to insufficient cooling of the platinum. Thus a water-cooled target was designed. This target was proven to be able to handle more than 30 TP per pulse. Fig. 6 shows the actual target after FY1996-1997 runs. There is no visible damage in the Platinum or in the Copper base. Detector upgrades were done in the following areas:

- Drift Chamber: The old jet chamber was replaced by the new Ultra Thin Chamber (UTC). The improvements are:
  1. Better Resolution: $\Delta P/P$ is now $\sim 1.4\%$, improved by a factor of 2.
  2. Less Material: The active region material reduced by a factor of 5. This gives less multiple scattering and better Z tracking.
- Scintillating Fiber Target: New scintillating fiber target improved the light output by factor of 2 and each fiber is instrumented with 500 MHz GaAs CCD digitizers.
- Pure CSI End cap: Both upstream and downstream end caps were replaced by pure CsI crystal [7]. The crystals are viewed by Hamamatsu high field mesh phototubes operated in a 10 kG magnetic field [8]. All 143 channels are viewed by the 500 MHz GaAs digitizers. The timing resolution of the end cap veto improved by more than factor of two over the old lead-scintillator end cap.
- DAQ System: Replace computer/tape drive and DAQ systems so the through put increased by factor of four.

5 Running Conditions

The 1995 running conditions were:

- Beam Flux
  1. Spill length/cycle time: Initial 7 weeks run with 1.2/3.2 sec and changeover to 1.6/3.6 sec in the last 10 Weeks. The effective spill length changed from 1.0 second to 1.35 seconds.
  2. K Flux: The LESBIII momentum was tuned at 790 Mev/c. The beam purity was $K^+/\pi^+ = 3$. With incident kaons 6.2 M/spill the stopping K rate was 1.2M/spill. (19% stopped). The typical proton beam on the 6 cm Pt target was 15 TP.
- Online Acceptance: The live time of the DAQ system was maintained at 73% . The online photon veto loss was 10%.
- Data: With a 25-week AGS run, the effective data taking time was 17 weeks. There were total of 4000 8 mm tapes analyzed, 150 million events. Total stopped kaons(KB), were 1.49×10^{12}.

6 Data Analysis and Results

As discussed in the experimental method section, we selected the kinematic region between $K^+ \to \pi^+\pi^0$ and $K^+ \to \mu^+\nu_\mu$. Still, we had to reject the background down to the 10^{-11} level. Fig. 7 shows the tools we used to reject the background. The two independent rejections allowed us to measure the residual background of each process. We used the data to study the rejection power. In this way, we could estimate the background from the data. Fig. 8. illustrates the process. First we selected photon-veto reversed events, *i.e.* those with evidence of a photon. This yielded two events in the signal box . From the data in the Kpi2 region, we measured the gamma rejection to be 46.6. This implied, N(background)=2/1.6/46.6=.003, the 1.6 factor is the additional rejection factor we could gain by imposing the TD fit which we did not apply for this study. With all the cuts applied, we calculated that the background from all sources to be 0.08 ± 0.03 event. Results from this analysis were published in [3]. In the final sample, one event is left in the $K^+ \to \pi^+\nu\bar{\nu}$ region. Fig. 9 shows the the range vs. kinetic energy plot for final $K^+ \to \pi^+\nu\bar{\nu}$ candidates, after a cut on momentum. The event in the signal box is far from the cut boundaries. Fig. 10 shows the event display: it is a very clean event. With one observed event, the branching ratio is determined by the total number of kaons stopped (1.49×10^{12}) corrected by the acceptance. Fig. 11, lists the acceptance factor of various cut. The total acceptance is .16 % . The branching ratio is calculated to be

$$\mathrm{BR}(\ K^+ \to \pi^+\nu\bar{\nu}\ ) = 4.2^{+9.7}_{-3.5} \times 10^{-10}$$

This is in statistical agreement with the expected range for this decay in the Standard Model, $(0.6 - 1.5) \times 10^{-10}$.

7 Acknowledgment

The E787 collaboration, which is responsible for the work presented here:
S. Adler, M.S. Atiya, I-H. Chiang, M. Diwan, J.S. Frank, J.S. Haggerty, S.H. Kettell, T.F. Kycia, K.K. Li, L.S. Littenberg, C. Ng, A. Sambamurti, A.J. Stevens, R.C. Strand and C.H. Witzig: *Brookhaven National Laboratory*
T. Komatsubara, M. Kuriki, N. Muramatsu, and S. Sugimoto: *KEK: Tanashi-branch*
T. Inagaki, S. Kabe, M. Kobayashi, Y. Kuno, T. Sato, T. Shinkawa, Y. Yoshimura: *KEK*
W.C. Louis: *Los Alamos National Laboratory*
Y. Kishi, T. Nakano and T. Sasaki: *Osaka University*
D.S. Akerib, M. Ardebili, M.R. Convery, M.M. Ito, D.R. Marlow, R.A. McPherson, P.D. Meyers, M.A. Selen, F.C. Shoemaker, A.J.S. Smith and J.R. Stone: *Princeton University*
P. Bergbusch, E.W. Blackmore, D.A. Bryman, L. Felawka, P. Kitching, A. Konaka,

J.A. Macdonald, J. Mildenberger, T. Numao, P. Padley, J-M. Poutissou, R. Poutissou, G. Redlinger, J. Roy, M. Rozon, R. Soluk and A.S. Turcot: *TRIUMF* This work was supported by the U.S. Department of Energy under contract no. DE-AC02-76CH00016.

References

1. S. L. Glashow, J. Iliopoulos, and L. Maiani, Phys. Rev. D 2 , 1285 (1970)

2. Rare decay modes of the K mesons in gauge theories. M. K. Gaillard and B. Lee. Phys. Rev. D 10 , 897 (1974)

3. S. Adler *et al.*, Phys. Rev. Lett. **79** , 2204, (1997)

4. J. H. Klem, R. H. Hildebrand and R. Stiening, Phys. Rev. D. 4, 66 (1971), D. C. Cable, R. H. Hildebrand, C. P. Pang, R. Stiening , Phys. Rev. D., 8, 3807, (1973).

5. Y. Asano, E. Kutani, S. Kurokawa, T. Miyachi, M. Miyajima, Y. Nagashima, T. Shinkawa, S. Sugimoto and Y. Yoshimura, Phys. Lett. **B107**, 159, (1981)

6. M. S. Atiya *et al.* Nucl. Instr. & Methods. **A321**, 129-151 (1992)

7. I-H. Chiang et al., IEEE Trans. Nucl. Sci. NS-42, 394-400, 1995.

8. T.K.Komatsubara *et al.* Nucl. Inst. & Methods. **A404**, 315-326, (1998)

K^+ Decays

M_K	493.68(2) MeV/c^2
τ_K	12.37(3) ns
decay mode	**BR**
$K^+ \to \mu^+\nu$	63.5%
$K^+ \to \pi^+\pi^0$	21.2%
$K^+ \to \pi^+\pi^-\pi^+$	5.6%
$K^+ \to \pi^0 e^+\nu$	4.8%
$K^+ \to \pi^0\mu^+\nu$	3.2%
$K^+ \to \pi^+\pi^0\pi^0$	1.7%
$K^+ \to \mu^+\nu\gamma$	0.5%
$K^+ \to \pi^+\nu\bar{\nu}$	(10^{-10})

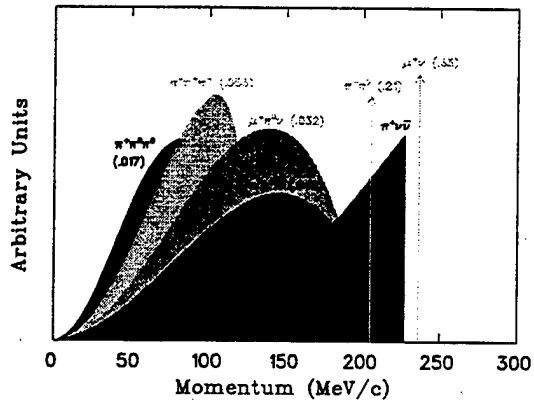

Figure 1: *The major decay modes.*

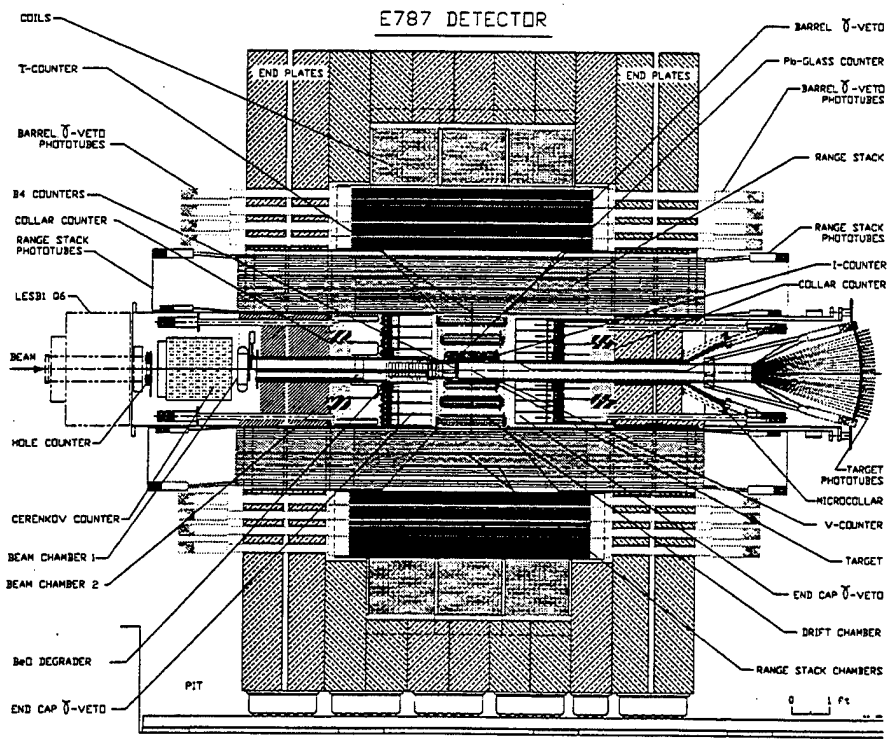

Figure 2: *The E787 detector.*

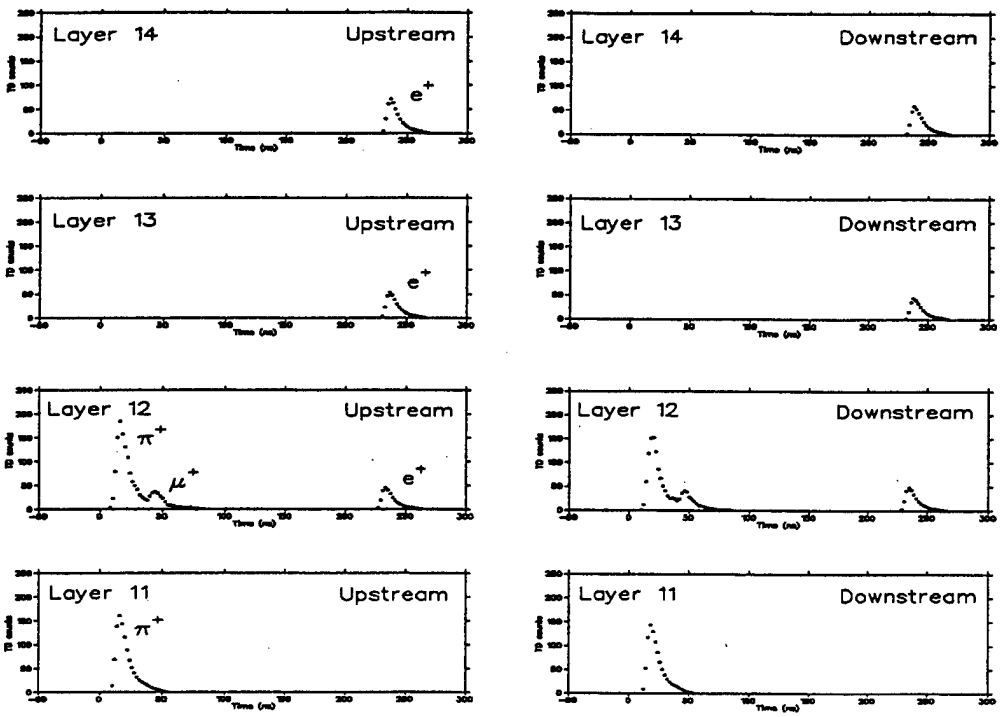

Figure 3: *The $\pi^+ \rightarrow \mu^+ \rightarrow e^+$ sequence.*

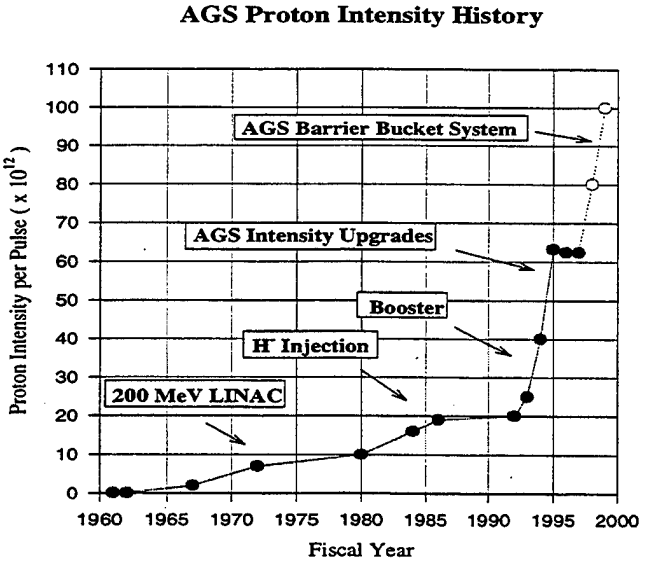

Figure 4: *The AGS intensity history*

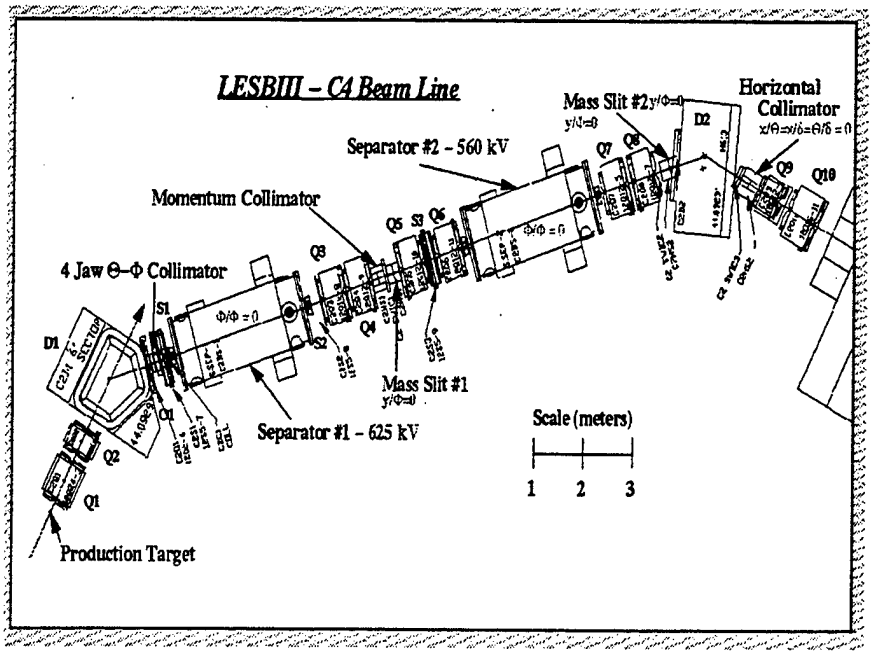

Figure 5: *The LESBIII (two stage separated beam)*

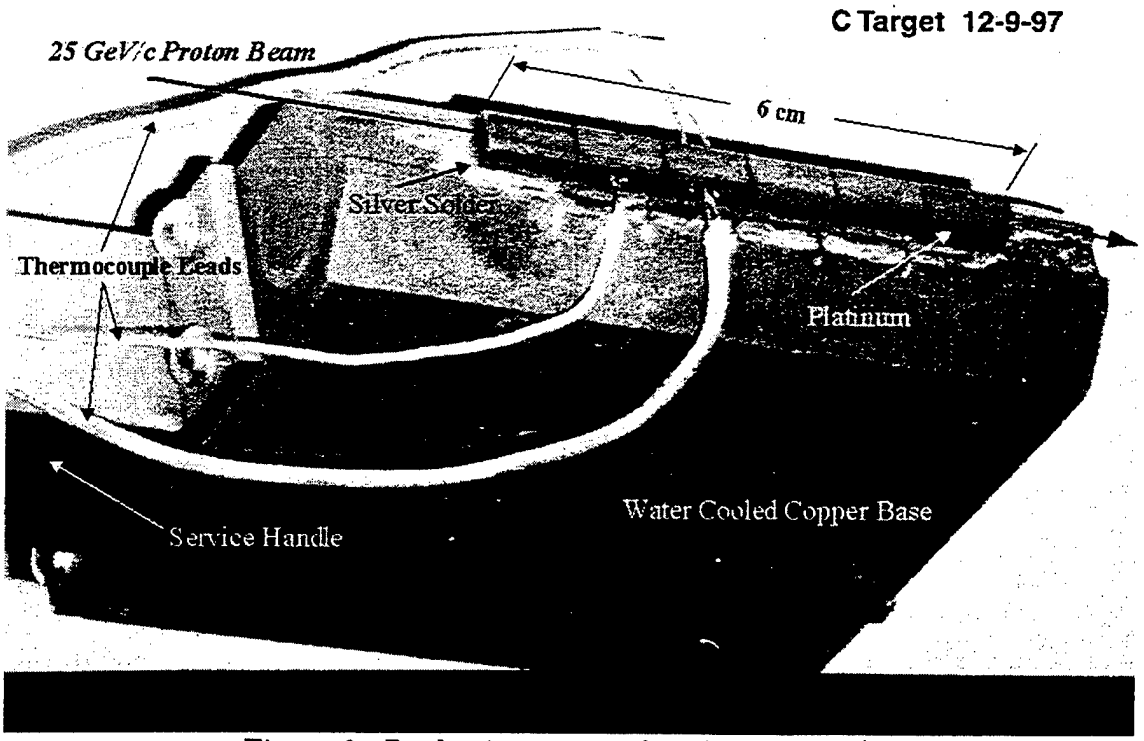

Figure 6: *Production target after the FY1996/97 run*

Backgrounds

	Background	Tools
$K^+ \to \mu^+ \nu_\mu$	μ mis-id	dE/dx, $\pi^+ \to \mu^+ \to e^+$
	kinematics wrong	E, P, R
$K^+ \to \mu^+ \nu_\mu \gamma$	μ mis-id	$\pi^+ \to \mu^+ \to e^+$
	1 photon missed	γ veto, branching ratio
$K^+ \to \pi^+ \pi^0$	2 photons missed	E, P, R, γ veto
	kinematics wrong	
Beam π's	mis-id as K decay	beam particle ID
	(mis-ID beam π as K	timing, beam dE/dx
	or accidental K with π)	extra beam track, bad vertex
$K^+ n \to K^0 p$	p,μ missed	target timing
$\hookrightarrow K_L \to \pi^+ l^- \nu$		target gaps
		extra particles

Figure 7: *Background rejection Tools*

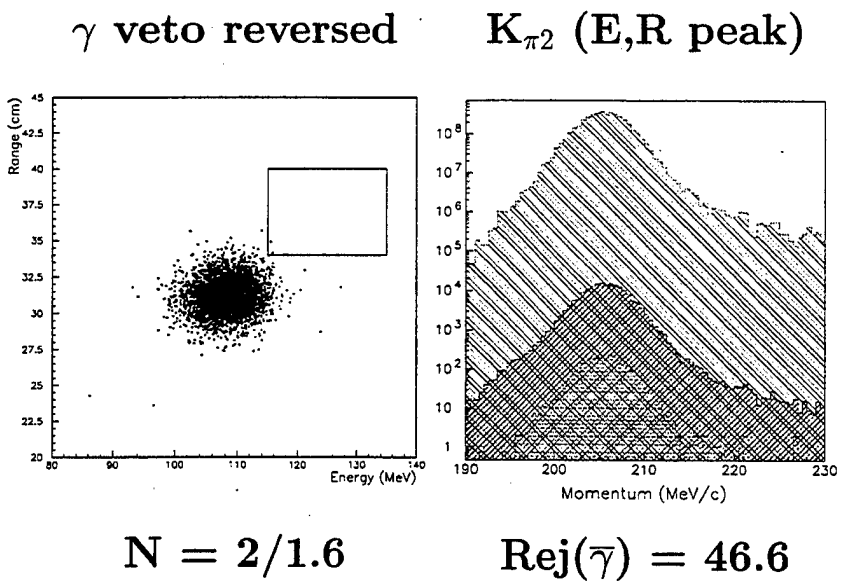

$N_{b.g.} = N_{Kin.}/R_{\bar{\gamma}} = 0.03$

Figure 8: $K^+ \to \pi^+ \pi^0$ *rejection.*

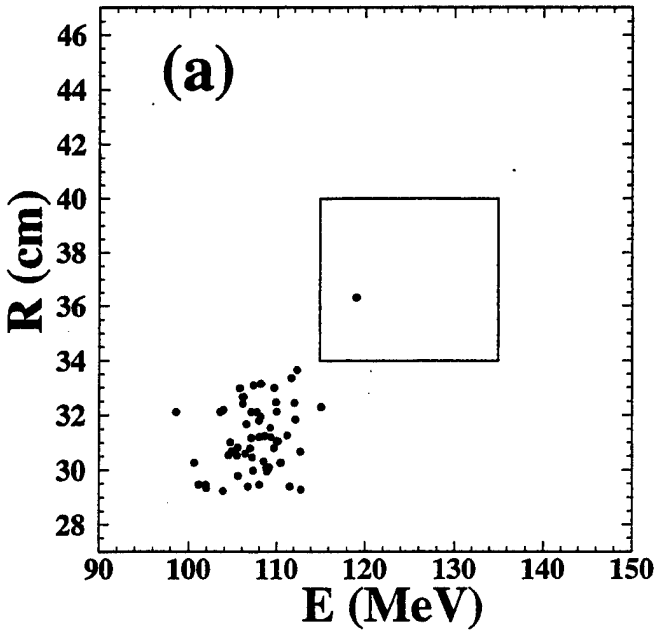

Figure 9: *Distribution of $K^+ \to \pi^+ \nu\bar{\nu}$ candidates after all cuts.*

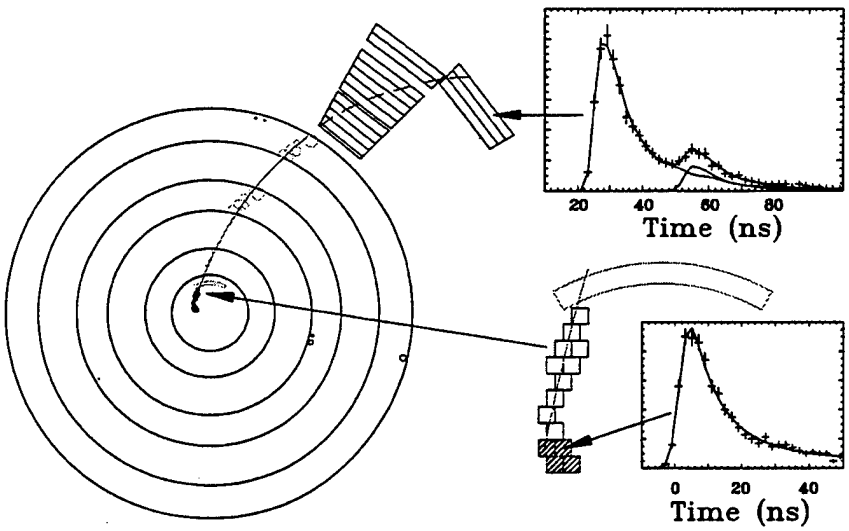

Figure 10: *The event display.*

Acceptance

Acceptance factors	method	
K^+ stop efficiency	BR($K_{\mu 2}$)	0.75
K^+ decay after 2 ns	$K_{\mu 2}$	0.813
$K^+ \to \pi^+ \nu\bar{\nu}$ phase space	MC	0.162
Solid angle acceptance	MC	0.386
π^+ nucl. int., decay-in-flight	MC	0.502
Reconstruction efficiency	$K_{\mu 2}$	0.956
Other kinematic constraints	π_{scat}	0.713
$\pi - \mu - e$ decay acceptance	π_{scat}	0.247
Beam and target analysis	$K_{\mu 2}$	0.659
Accidental loss	$K_{\mu 2}$	0.747
Total acceptance		0.0016(1)

Check by measuring BR($K^+ \to \pi^+\pi^0$)

BR($K^+ \to \pi^+\pi^0$)=0.202 $\pm$ 0.009 (e787)
(0.2116 $\pm$ 0.0014 PDG)

Total 1.49×10^{12} K^+ stops recorded

$$\mathrm{BR}(K^+ \to \pi^+ \nu\bar{\nu}) = 4.2^{+9.7}_{-3.5} \times 10^{-10}$$

Figure 11: *The results*

DISCLAIMER

Report Number (14) BNL--65258
CONF-9710190--

Publ. Date (11) 199802
Sponsor Code (18) DOE/ER, XF
UC Category (19) UC-414, DOE/ER

DOE